*Progress In Electromagnetics Research C, Vol. 66, 39–46, 2016*

# High Efficiency and High Power Staggered Double Vane TWT Amplifier Enhanced by Velocity-Taper Design

**Xianbao Shi[1, 2], Laxma R. Billa[1], Yubin Gong[2], Muhammad N. Akram[1], and Xuyuan Chen[1, *]**

**Abstract**—Previously reported staggered double vane (SDV) slow wave structure (SWS) traveling wave tube (TWT) gave electron efficiency as low as 3.4% at 220 GHz, which needs to be improved. One easy method to improve the electron efficiency and the output power is to reuse the spent electron beam energy, by resynchronizing electron velocity to the phase velocity of the terahertz (THz) signal at the second section of the TWT. In this article, we have modified the pitch of the SWS to realize the tapered phase velocity, which is for the first time, to our knowledge, applied to the SDV SWS at 220 GHz. By varying the geometry configuration, an optimized structure of tapered pitch SWS has been successfully developed. The results reported in this paper show a significant improvement of the output power, gain and electron efficiency. At 220 GHz, the output power has increased by about 65% with respect to the previous reported value reaching 111 W, and the electron efficiency has improved from 3.4% to 5.6%. In order to simplify the microfabrication process, an input/output coupler with $E$-plane bending has been designed, which can be fabricated by using only one mask UV-LIGA process.

## 1. INTRODUCTION

Wide-band high-power terahertz (THz) radiation sources developed by the vacuum electronics technology are attractive for many applications, such as high-data-rate communication, imaging and space applications [1–4]. Traveling-wave tube (TWT) is one of the most important THz wave vacuum electronics devices due to its outstanding performance in bandwidth, power capacity (power per volume) and high output power. As the core part, a slow-wave structure (SWS) critically determines the performance of the TWT. In recent years, some studies have focused on staggered double vane (SDV) SWS in the terahertz and millimeter wave TWTs and back wave oscillators (BWOs) [5–7], which has a sheet electron beam tunnel. As well known, the sheet beam can theoretically provide a large current with small space charge field owing to the beam horizontal extensibility, which enables the TWT to generate high power for both millimeter and terahertz radiations [8, 9].

The SDV SWS was first designed by Shin et al. with operating voltage of 20 kV and current of 250 mA. They achieved an output power of 150 W at 220 GHz, but the current density was as high as 357 A/cm$^2$, which is very difficult to be focused over a long distance of the tube. So, their sheet beam transmission was only about 73.6% [10–12], while the electron efficiency was only about 3%. Recently, Shi et al. improved the performance of the 220 GHz SDV TWT by introducing a newly designed periodical cusped magnet (PCM) system [13]. With a current density of 200 A/cm$^2$, a 100% sheet beam transmission was achieved in a 75 mm length drift tube. The output power was 67.28 W with the operating voltage of 25 kV and beam current of 80 mA.

*Received 3 May 2016, Accepted 5 July 2016, Scheduled 14 July 2016*

* Corresponding author: Xuyuan Chen (Xuyuan.Chen@hbv.no).

[1] Department of Micro- and Nano-system Technology (IMST), University College of Southeast Norway, Borre 3184, Norway.

[2] Vacuum Electronics National Laboratory, School of Physical Electronics, University of Electronic Science and Technology of China, Chengdu 610054, China.

The design reported in [13] shows a shortcoming as the electron beam energy is wasted in the second portion of the TWT, where the high phase velocity of the THz signal is mismatched to the slowed down velocity of the electron beam. To increase the efficiency and the output power of the TWTs by reusing the spent electron beam energy, tapered phase velocity method can be employed [14]. Bo et al. demonstrated a large beam tunnel 220 GHz folded waveguide (FWG) TWT by tapered phase velocity to promote output power by 30.4% from 79 W to 103 W [15]. However, as an important SWS, the SDV SWS with the tapered pitch design for modulate the phase velocity has not been reported so far. Another method, which has the potential for generating higher power at millimeter and sub-millimeter wave band by enlarging the beam power, is the multi-beam technology [16, 17]. We will not discuss this method in this article.

In this paper, we have investigated the design of high power TWT by developing tapered pitch SWS. Comparing TWT with uniform pitch SWS operating at center frequency of 220 GHz, the output power of the TWTs with one-step tapered pitch SWS and two-steps tapered pitch SWS were improved by 45.7% and 65%, respectively. In order to fabricate the designed TWT with the features of micro dimension, the key process of Micro-electromechanical Systems (MEMS) technology must be developed. Different from traditional design, a novel configuration of the input/output coupler, e.g., an $E$-plane bending input/output coupler has been designed to be compatible with UV-LIGA fabrication process.

This paper is organized in five parts. The modified SDV TWT with $E$-plane bending input/output coupler for simple MEMS fabrication is described in Section 2. In Section 3, we give the optimization results of the SDV TWT with $E$-plane bending and uniform pitch SWS. The tapered phase velocity scheme is studied in detail in Section 4, including the detailed design process, the performance of the TWT with tapered SWS and the improvement achieved. Finally, conclusions are drawn in Section 5.

## 2. DESIGN CHALLENGE AND SOLUTION

A typical SDV TWT is shown in Figure 1, which includes a SDV SWS with the 1st and the 2nd sections, transition structure, attenuator, the ridge-loaded input/output coupler, and the beam tunnel [13]. The purpose of placing an attenuator between the 1st and the 2nd section of SWS is to prevent the backward wave oscillations. The transition structure and the ridge-loaded waveguide are used for mitigating the reflections at the input and the output ports. It will help feed the THz signal into the SWS and lead the enlarged signal out of the SWS gently.

In the THz band, the structure dimension goes down to micrometer level, which cannot be fabricated by the traditional machining technology. Thereby, the MEMS technology is suitable to fabricate such structure. However, as shown in Figure 1, this ridge-loaded waveguide is contained with both high-transition ridge and 90° right-angle bending ridge, which cannot be realized with MEMS technology of a simple process flow. Moreover, the input/output coupler and the SDV SWS in this design have to be assembled together to make the whole structure. Therefore, it is very complicated to fabricate this structure using the MEMS technology.

For overcoming the disadvantages in Figure 1, a modified TWT with $E$-plane bending input/output coupler is proposed as shown in Figure 2, which is 90° bending of broader side of the waveguide. With this modified design, the SDV SWS can be fabricated easily with only one mask and one electroplating growth step in the $x$-direction, (see the inserted coordinate system). The optimized simulation results for this SDV TWT will be discussed in the next section.

## 3. UNIFORM PITCH SDV TWT WITH $E$-PLANE BENDING INPUT/OUTPUT COUPLER PERFORMANCE OPTIMIZATION

The design of the uniform pitch SDV TWT with $E$-plane bending input/output coupler has been optimized by numerical simulation. There are 45 pitches in the 1st section, 50 pitches in the 2nd section and 5 pitches for loading the attenuator, which have been determined as the optimized design to obtain the maximum output power. The performance, such as the dispersion characteristics of the SDV SWS, phase velocity of the travelling wave, the voltage standing wave ratio (VSWR) of the input/output port, and output power, have been investigated.

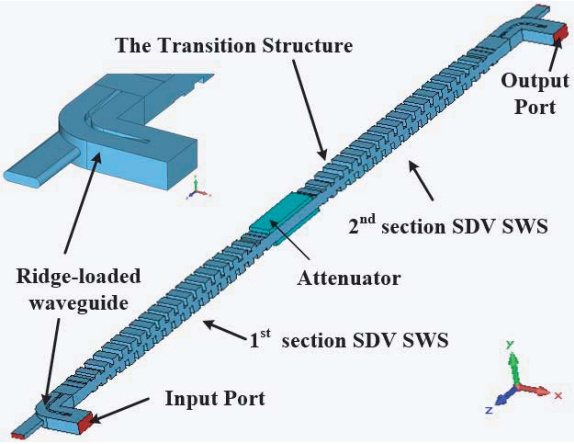


**Figure 1.** Typical SDV TWT with ridge-loaded input/output coupler.

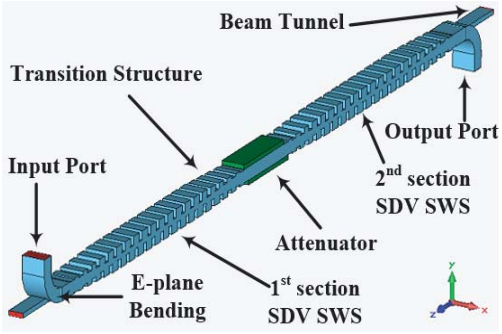


**Figure 2.** SDV TWT with $E$-plane bending input/output coupler.

Figure 3 shows the dispersion characteristics of the uniform pitch SDV TWT, which is obtained numerically by high frequency structure simulator (HFSS) software. An optimized 24.93 kV beam line is intercepting the first harmonic of the fundamental mode, which indicates the operating mode for the beam-wave interaction. It is clearly seen that in the frequency range of 200 GHz $\sim$ 250 GHz, there is a good synchronization between the beam-line and the dispersion curve.

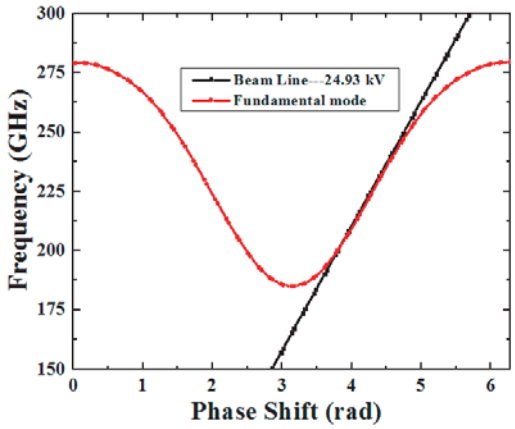


**Figure 3.** Dispersion characteristics of the uniform pitch SDV SWS.

By using HFSS, we also got the phase velocity *versus* frequency of travelling wave with respect to different pitch lengths of the uniform pitch SDV SWS, which is shown in the Figure 4. It can be seen that for the reduced pitch length from 0.540 mm to 0.533 mm, the phase velocity of the traveling wave decreases a little. The normalized phase velocity at 220 GHz will be changed from 0.298 to 0.294. The operating bandwidth defined by the flat form of the cure in Figure 4 changes slightly.

The voltage standing wave ratio (VSWR) of the input/output port is studied with Computer Simulation Technology (CST) Microwave Studio software, as shown in Figure 5. The farther the VSWR is from unity, the bigger the reflection will be. It can be observed that the VSWR is less than 2 in the operating frequency band, especially less than 1.5 from 200 GHz to 230 GHz, which means this input/output coupler has a low reflection that can ensure the suppression of self-excited oscillation.

Operating with the optimized beam voltage of 24.93 kV, beam current of 0.08 A and current density of 200 A/cm$^2$, the output power of the uniform pitch SDV TWT operating at 220 GHz is simulated by

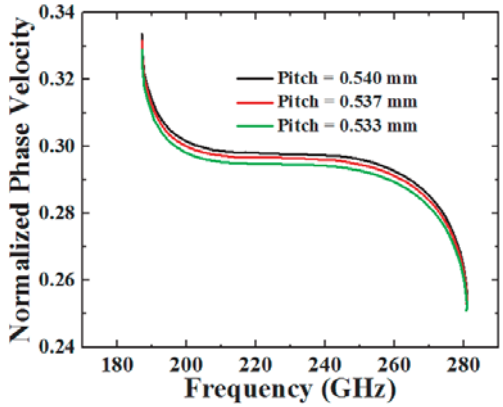


**Figure 4.** Normalized phase velocity of traveling wave with different pitch length.

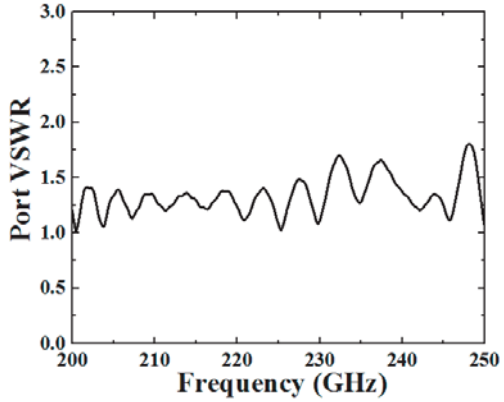


**Figure 5.** VSWR of the input/output port.

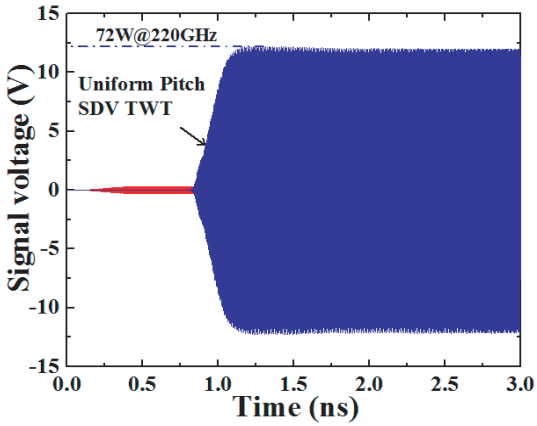


**Figure 6.** Output signal of the uniform pitch SDV TWT with *E*-plane bending input/output coupler.

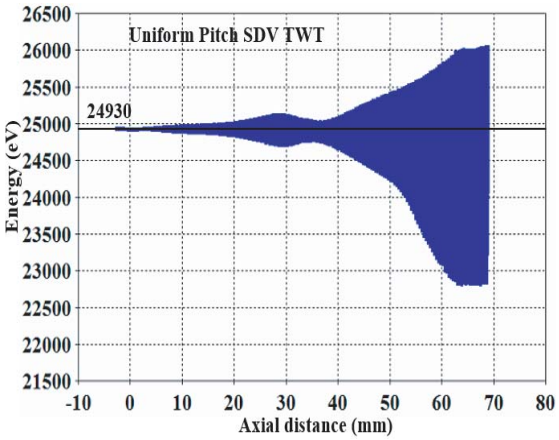


**Figure 7.** Phase space plot of the electrons in the pitch SDV TWT.

CST particle in cell (PIC) studio program. From Figure 6 we find that for this optimized design, after 1.5 ns interaction time, the output power is stable at 72 W, which gives an electron efficiency about 3.6% when input power is 50 mW. During the simulation study, we consider the copper surface with idea smoothness and the copper conductivity being 5.8e7 S/m, which are similar to that in the previous reported article [13].

Figure 7 illustrates the phase space plot of the electrons in the uniform pitch SDV TWT. As can be seen, at the end of the uniform pitch SDV TWT, the energy of the electron is decreased from 24930 eV to 22800 eV. However, due to the low electron efficiency, there will be a good potential to harvest electron energy at 22800 eV level for further amplifying the wave energy. In the next section, tapered pitch SDV SWS scheme is studied for reusing the spent electrons energy.

## 4. PHASE VELOCITY TAPER FOR IMPROVING OUTPUT POWER

For the uniform pitch SDV SWS, the phase velocity of the signal is synchronized with the electron beam velocity in the 1st section (see Figure 2), and the beam-wave interaction will take place effectively. As the electron beam gives the energy to the signal continuously, the velocity of the electron will decrease incessantly. Finally, the synchronization condition willbe breakdown in the 2nd section. In order to resynchronize the phase velocity with the used electron beam velocity, we have to modulate the

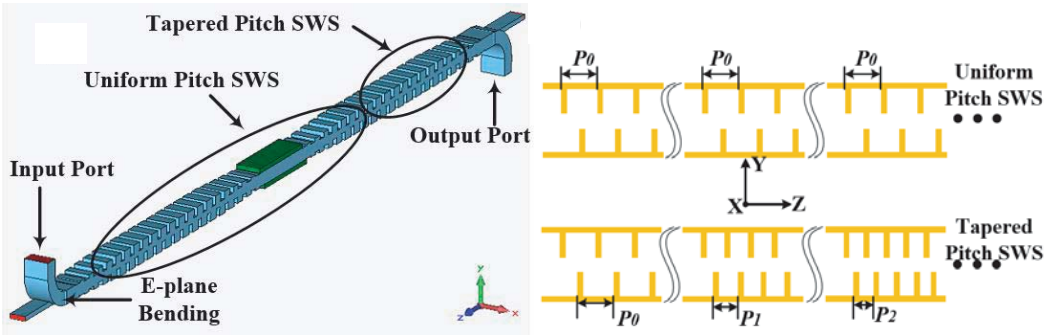


(a) (b)

**Figure 8.** (a) *E*-plane bending SDV TWT with tapered pitch SWS scheme, (b) schematic diagram of the uniform pitch SWS (top) and tapered pitch SWS (bottom).

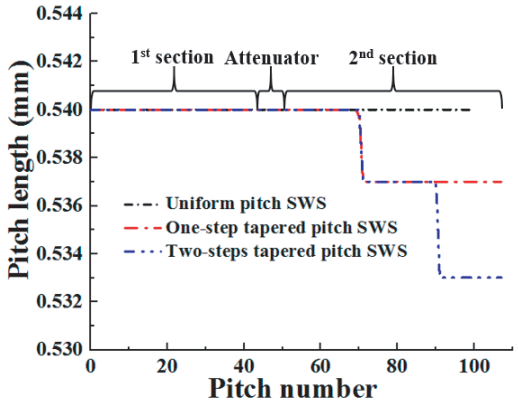


**Figure 9.** Pitch profile of the tapered pitch SDV SWS.

phase velocity, which can be done by adjusting the pitch of the 2nd section of the SDV SWS. After the resynchronization, the effective beam-wave interaction can continue for transferring more electron energy to the wave. Figure 8(a) shows the modified *E*-plane bending SDV TWT combined with the tapered pitch scheme. For a clear illustration, the schematic diagram of the uniform pitch SDV SWS and tapered pitch SDV SWS are enlarged in the Figure 8(b).

Figure 9 illustrates the pitch profile of the tapered pitch SDV SWS. As afore-described in Figure 4, the phase velocity of the traveling wave can be adjusted by changing the pitch length. Both one-step and two-steps tapered pitch are designed in the 2nd section of the SDV SWS. For the one-step tapered pitch design, the tapered pitch of 0.537 mm begins from the 20th period to the end of the 2nd section. For the two-steps tapered pitch design, the first tapered pitch of 0.537 mm begins from the 20th period to 39th period and the second tapered pitch of 0.533 mm begins from the 40th period to the end of the 2nd section of the SDV SWS.

Figure 10 depicts the electron energy *versus* axial distance for the one-step and the two-steps tapered pitch SDV TWTs operating at frequency 220 GHz, with the same beam parameters as the uniform pitch SDV TWT. As the beam-wave interaction is proceeding in the 2nd section of the SDV SWS with tapered pitch design, the energy of electron is decreased and transferred to the traveling wave. Moreover, at the end of the SDV TWT, energy of electrons is no more decreased, which means saturation of beam-wave interaction has reached.

By comparing Figure 7 and Figure 10, we can see that the electrons energy of the TWT with one-step tapered pitch SDV SWS can be decreased from 24930 eV to 22400 eV, while that with uniform pitch SDV SWS can only be decreased from 24930 eV to 22800 eV. Furthermore, the decreased energy of the electrons with two-steps tapered pitch SDV SWS is from 24930 eV to 22000 eV. Therefore, more

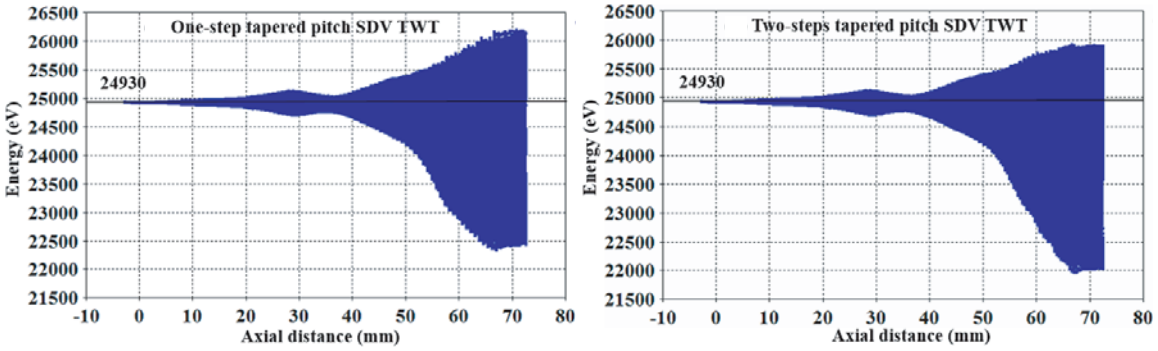


**Figure 10.** Phase space plot of the electrons in the SDV TWTs: (a) with one-step tapered pitch SDV SWS, (b) with two-steps tapered pitch SDV SWS.

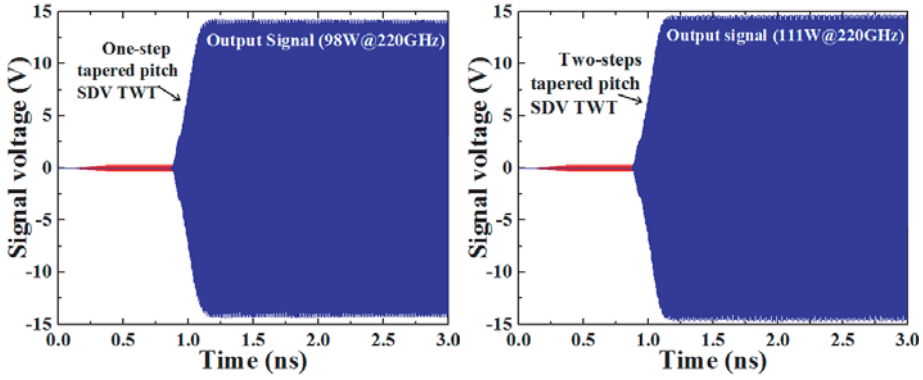


**Figure 11.** Output signal voltage of SDV TWTs: (a) with one-step tapered pitch SDV SWS and (b) two-steps tapered pitch SDV SWS.

beam power will be delivered to the traveling wave for the SDV TWT with two-steps tapered pitch design. The results show that with tapered pitch scheme, resynchronizing the phase velocity and the electron velocity can be achieved in the 2nd section of the SDV SWS.

In Figure 11, we compare the output signal voltage of the SDV TWTs with one-step tapered pitch SDV SWS and with two-steps tapered pitch SDV SWS. When the input power is 50 mW, the output power of the SDV TWT with one-step tapered pitch design and two-steps tapered pitch design are found equal to 98 W and 111 W respectively, corresponding gains are 32.9 dB and 33.5 dB respectively. Comparing with previous published results [13], at 220 GHz, the output power of the SDV TWT with two-steps tapered pitch design has been increased by about 65%, and the electron efficiency has been improved from 3.4% to 5.6%.

After detailed simulations by CST PIC Studio, the output power and its improvement of the two-steps tapered pitch SDV TWT and referenced SDV TWT are shown in Figure 12. It can be observed that the maximum output power of the two SDV TWTs is both at about 213 GHz instead of 220 GHz, which is due to the fact that the interaction impedance increases as the operation frequency goes down [13]. However, at both edges of operating frequency band, the synchronization condition will be broken, the interaction efficiency thus decreases, which leads to diminished output power. We can also see that at the center frequency of 220 GHz, the output power improvement is as high as 65%. Moreover, the improvement is more than 50% in the whole operating frequency band.

For easy comparison, the performance of the above mentioned four types of SDV TWTs operating at 220 GHz is described in Table 1.

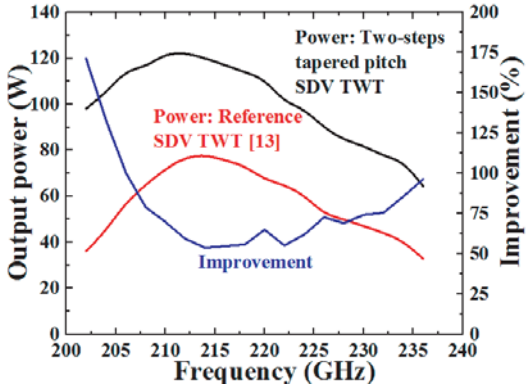


**Figure 12.** The output power *versus* the operation frequency for two-steps tapered pitch SDV TWTs and referenced SDV TWT [13]. The improvement in percentage is also shown.

**Table 1.** Performance of the four types TWTs @220 GHz.

| Taper information | SDV TWT reported in Reference [13] | SDV TWT with Uniform pitch SWS | SDV TWT with One-step tapered pitch SWS | SDV TWT with Two-steps tapered pitch SWS |
|---|---|---|---|---|
| Beam voltage | 25000 V | 24930 V | 24930 V | 24930 V |
| Beam current | 80 mA | 80 mA | 80 mA | 80 mA |
| Input power | 50 mW | 50 mW | 50 mW | 50 mW |
| Output power | 67.28 W | 72 W | 98 W | 111 W |
| Gain | 31.29 dB | 31.58 dB | 32.92 dB | 33.46 dB |
| Average beam efficiency | 3.4% | 3.6% | 4.9% | 5.6% |
| Output power improvement | Reference | 7% | 45.7% | 65% |

## 5. CONCLUSION

In this article, the output power of the SDV TWT with uniform pitch SWS and operating at 220 GHz is improved from 67.28 W to 72 W, with optimized operating parameters.

For further increasing the output power and conversion efficiency, tapered phase velocity scheme is successfully applied in the SDV TWT. Two TWTs, one with one-step tapered pitch SWS and the other with two-steps tapered pitch SWS, are optimized. Output power can be enhanced to 111 W at the central frequency of 220 GHz. An improvement of 65% is obtained for the two-steps tapered pitch scheme. The conversion efficiency is increased to 5.6%. The results show that in the frequency range from 202 GHz to 236 GHz, the improvement will be more than 50%. Moreover, the maximum output power of the TWT with two-steps tapered pitch SWS is 122.5 W at 212 GHz, corresponding to a gain of 33.9 dB and conversion efficiency of 6.14%.

For simplifying the fabrication process, the TWT is modified with an $E$-plane bending input/output coupler, which is more suitable for the MEMS fabrication technology. For future work, detailed microfabrication and measurement of the best designed two-steps tapered pitch SDV TWT are under consideration.

## ACKNOWLEDGMENT

This work is supported in part by the Norwegian Micro- and Nano-fabrication facility NorFab (197411/V30), National Natural Science Foundation of China (61531010), Key Laboratory Foundation (2014-764.XY.K), and China Scholarship Council (No. 20150607006).

## REFERENCES

1. Booske, J. H., "Plasma physics and related challenges of millimeter-wave-to-terahertz and high power microwave generation," *Phys. Plasmas*, Vol. 15, No. 5, 055 502-1–055 502-16, May 2008.
2. Borsuk, G. M. and B. Levush, "Vacuum electronics research perspective at the naval research laboratory," *IEEE Int. Vacuum Electron. Conf.*, 3, Monterey, USA, May 21–24, 2010.
3. Tucek, J., M. Basten, D. Gallagher, and K. Kreischer, "Sub-millimeter and THz power amplifier development at Northrop Grumman," *IEEE Int. Vacuum Electron. Conf.*, 19, Monterey, USA, May 21–24, 2010.
4. Siegel, P. H., "Terahertz technology," *IEEE Trans. Microw. Theory Tech.*, Vol. 50, No. 3, 910–928, 2002.
5. Shin, Y. M., A. Baig, L. R. Barnett, W. C. Tsai, and N. C. Luhmann, "System design analysis of a 0.22-THz sheet-beam traveling-wave tube amplifier," *IEEE Transactions on Electron Devices*, Vol. 59, No. 1, 234–240, 2012.
6. Shin, Y. M., A. Baig, L. R. Barnett, N. C. Luhmann, J. Pasour, and P. Larsen, "Modeling investigation of an ultrawideband terahertz sheet beam traveling-wave tube amplifier circuit," *IEEE Transactions on Electron Devices*, Vol. 58, No. 9, 3213–3218, 2011.
7. Xu, X., Y. Wei, F. Shen, Z. Duan, Y. Gong, H. Yin, and W. Wang, "Sine waveguide for 0.22-THz traveling-wave tube," *IEEE Electron Device Letters*, Vol. 32, 1152, 2011.
8. Booske, J. H., R. J. Dobbs, C. D. Joye, et al., "Vacuum electronic high power terahertz sources," *IEEE Transactions on Terahertz Science and Technology*, Vol. 1, No. 1, 54–75, 2011.
9. Booske, J. H., B. D. Mcveya, and T. M. Antonsen, "Stability and confinement of nonrelativistic with periodic cusped magnetic focusing," *J. Appl. Phys.*, Vol. 73, No. 9, 4140–4155, 1993.
10. Shin, Y. M., L. R. Barnett, and N. C. Luhmann, "Phase-shifted traveling-wave-tube circuit for ultrawideband high-power submillimeter-wave generation," *IEEE Transactions on Electron Devices*, Vol. 56, No. 5, 706–712, 2009.
11. Shin, Y. M., A. Baig, L. R. Barnett, N. C. Luhmann, J. Pasour, and P. Larsen, "Modeling investigation of an ultrawideband terahertz sheet beam traveling-wave tube amplifier circuit," *IEEE Transactions on Electron Devices*, Vol. 58, No. 9, 3213–3218, 2011.
12. Shin, Y. M., A. Baig, L. R. Barnett, W. C. Tsai, and N. C. Luhmann, "System design analysis of a 0.22-THz sheet-beam traveling-wave tube amplifier," *IEEE Transactions on Electron Devices*, Vol. 59, No. 1, 234–240, 2012.
13. Shi, X., Z. Wang, X. Tang, T. Tang, H. Gong, Q. Zhou, W. Bo, Y. Zhang, Z. Duan, Y. Wei, Y. Gong, and J. Feng, "Study on wideband sheet beam traveling wave tube based on staggered double vane slow wave structure," *IEEE Trans. Plasma Sci.*, Vol. 42, No. 12, 3996–4003, 2014.
14. Ghosh, T. K., A. J. Challis, A. Jacob, and D. Bowler, "Design of helix pitch profile for broadband traveling-wave tubes". *IEEE Transactions on Electron Devices*, Vol. 56, No. 5, 1135–1140, 2009.
15. Bo, W., Q. Zhou, Y. Zhang, and X. Shi, "Research on 0.22 THz folded-waveguide traveling-wave tube with a proper phase-velocity taper," *IEEE International Vacuum Electronics Conference*, 4–5, 2015.
16. Gong, Y., H. Yin, L. Yue, Z. Lu, Y. Wei, J. Feng, Z. Duan, and X. Xu, "A 140-GHz two-beam overmoded folded-waveguide traveling-wave tube," *IEEE Transactions on Electron Devices* Vol. 39, 847, 2011.
17. Nguyen, K., L. Ludeking, J. P. D. Pershing, E. Wright, D. K. Abe, and B. Levush, "Design of terahertz Extended Interaction Klystrons," *IEEE Int. Vacuum Electron. Conf.*, 23, Monterey, USA, May 21–24, 2010.